The Tetranuclear Manganese Cluster in Photosystem II: Location and Magnetic Properties of the S_2 State As Determined by Saturation−Recovery EPR Spectroscopy†

Dionysios Koulougliotis,‡ Robert H. Schweitzer, and Gary W. Brudvig*

Department of Chemistry, Yale University, New Haven, Connecticut 06520-8107

Received February 12, 1997; Revised Manuscript Received May 28, 1997⊗

ABSTRACT: The spin−lattice relaxation enhancement of the dark-stable tyrosine radical, $Y_D^•$, by the S_2 state of the O_2-evolving complex (OEC) of photosystem II (PSII) has been measured by using saturation−recovery EPR spectroscopy. Two forms of the S_2 state have been compared: the multiline EPR signal species in untreated PSII and the altered multiline EPR signal species in NH_3-treated PSII. Previous work has shown that the non-single-exponential spin−lattice relaxation kinetics of $Y_D^•$ in S_2-state PSII result from a dipole−dipole interaction with the Mn_4 cluster of the OEC. By taking into account the temperature variation of the effective magnetic moment of the S_2-state multiline EPR signal form of the OEC, we provide a quantitative analysis of its temperature-dependent enhancement of the spin−lattice relaxation of $Y_D^•$. Different spin states of the Mn_4 cluster in the S_2 state are responsible for the effect at different temperature regimes: for $T \leq 10$ K, it is the ground spin state ($S = {}^1/_2$); for $T \geq 30$ K, it is the first excited spin state; and at intermediate temperatures, the contributions of the two spin states are comparable. The relaxation enhancement of $Y_D^•$ is equivalent for both forms of the S_2-state multiline EPR signal examined, indicating that the magnetic properties of the Mn_4 cluster are very similar in the S_2 state for both untreated and NH_3-treated PSII. EPR progressive microwave-power saturation has also been used to assess the spin−lattice relaxation properties of the Mn_4 cluster giving the altered S_2-state multiline EPR signal in the NH_3 derivative of PSII. The Orbach mechanism is shown to provide the dominant relaxation pathway; the energy difference between the ground and first excited spin states is estimated to be 30 ± 2 cm^{-1}, which is very similar to the value found for the S_2-state multiline EPR signal species in untreated PSII. Below 4 K, the effectiveness of the S_2-state multiline EPR signal species as a spin relaxation enhancer of $Y_D^•$ drops dramatically. This is interpreted to occur because of temperature-dependent ^{55}Mn nuclear spin−lattice relaxation which causes averaging of the effective Larmor frequency of the S_2-state multiline EPR signal species during the time scale for spin−lattice relaxation of $Y_D^•$; because the line shape of the S_2-state multiline EPR signal is dominated by isotropic ^{55}Mn nuclear hyperfine splittings, such nuclear relaxation processes allow frequencies in near resonance with that of $Y_D^•$ to be accessed, thereby producing a greater relaxation enhancement. By using a dipolar model that includes the line shapes of both the $Y_D^•$ and S_2-state multiline EPR signals, the spin−lattice relaxation enhancement of $Y_D^•$ is analyzed to obtain a lower limit of 22 Å for the distance between $Y_D^•$ and the OEC. Together with recent studies showing a close proximity of the Mn_4 cluster to $Y_Z^•$, these results provide further support for an asymmetric location of the Mn_4 cluster with respect to the two redox-active tyrosines in PSII.

The O_2-evolving complex (OEC) of photosystem II (PSII) catalyzes the light-driven four-electron oxidation of water to O_2 by advancing through five intermediate-oxidation states known as S_i states ($i = 0-4$). In the dark, the S_0 and S_1 states are the most stable (Kok et al., 1970). Upon long-term dark adaptation, however, S_0 is slowly oxidized to S_1 (Vermaas et al., 1984) by a mechanism described by Styring and Rutherford (1987). The S_2 and S_3 states are unstable in the dark and decay back to the S_1 state (Rutherford et al., 1992, and references cited therein). The S_4 state is a transient intermediate that spontaneously forms the S_0 state with the concomitant release of O_2. Although it is known that four Mn ions are required for O_2 evolution (Cheniae & Martin, 1970; Yocum et al., 1981; Murata et al., 1984), the structure and location of the complex responsible for the water-oxidation chemistry are still under debate.

The S_2 state gives rise to two types of Mn EPR signals referred to as the multiline and $g = 4.1$ signals, respectively. At X band (9 GHz), the $g \approx 2$ multiline EPR signal displays 19 or more partially-resolved Mn hyperfine lines, with an average splitting of about 85 G (Dismukes & Siderer, 1981; Hansson & Andréasson, 1982). The multiline EPR signal has also been examined at S band (3.9 GHz), where it exhibits 40−50 hyperfine lines with an average separation of about 25 G (Haddy et al., 1989), as well as at Q band (34 GHz) (Hansson et al., 1987; Åhrling & Pace, 1995). The results of the spectroscopic characterization of the S_2-state multiline EPR signal can be summarized as follows. The signal amplitude shows Curie-law behavior for temperatures higher than 1.4 K, indicating that it arises from an $S = {}^1/_2$

† This work was supported by the National Institutes of Health (GM32715 and GM36442).

* Corresponding author.

‡ Present address: Department of Chemistry, University of Florence, Via Gino Capponi 7, 50121, Florence, Italy.

⊗ Abstract published in *Advance ACS Abstracts,* August 1, 1997.

S0006-2960(97)00326-7 CCC: $14.00

ground spin state (Aasa et al., 1987; Britt et al., 1992). Progressive microwave-power saturation experiments (Hansson et al., 1984; de Paula & Brudvig, 1985; Pace et al., 1991) as well as analyses of the temperature dependence of the line width (Hansson et al., 1987) have favored the Orbach process as the dominant spin−lattice relaxation pathway for the multiline EPR signal species. Direct measurement of the electron spin−lattice relaxation rate of the multiline EPR signal species as a function of temperature (Lorigan & Britt, 1994) confirmed that the species relaxes via the Orbach process involving an excited spin-state manifold 36.5 ± 0.7 cm^{-1} above the ground state. The orientation dependence of the multiline EPR signal has been examined at both X (Rutherford, 1985; Kim et al., 1992) and S bands (Haddy et al., 1989), showing significant anisotropy, especially in the latter. This has been primarily attributed to hyperfine anisotropy which is consistent with the studies done at Q band (Hansson et al., 1987; Åhrling & Pace, 1995) that indicate the absence of significant *g*-anisotropy.

The S_2-state multiline EPR signal can be detected in several modified forms upon treatment with ammonia (Beck & Brudvig, 1986; Beck et al., 1986), upon exchange of Ca^{2+} with Sr^{2+} (Boussac & Rutherford, 1988) or by Ca^{2+}-depletion (Boussac et al., 1989). In all cases, the hyperfine spacing is reduced and the number of resolved hyperfine lines is increased. The effect of variations of the Heisenberg exchange parameters upon the Mn cluster transformation has been shown to explain qualitatively these modifications of the S_2-state multiline EPR signal (Belinskii, 1994).

In addition to the multiline EPR signal, there exists a second EPR signal centered at $g = 4.1$ which has been assigned to an alternate form of the S_2 state. It has a width of 320−360 G and lacks resolved hyperfine structure. However, at least 16 partially resolved hyperfine lines, spaced by about 36 G, have been observed on the $g = 4.1$ signal in oriented NH_3-treated PSII membranes (Kim et al., 1990, 1992). This result provided direct experimental support for the suggestion made earlier by de Paula et al. (1985, 1986) and Zimmermann and Rutherford (1986) that the $g = 4.1$ signal arises from a multinuclear Mn complex. According to the same proposal, the $g = 4.1$ form of the Mn cluster can be converted into the form exhibiting the multiline EPR signal upon a temperature-dependent structural rearrangement.

The spin state giving rise to the $g = 4.1$ S_2-state EPR signal remains controversial. Initial EPR studies suggested an $S = {}^3/_2$ state, even though it was not agreed on whether it is a ground (de Paula et al., 1986; Hansson et al., 1987) or a first excited state (Pace et al., 1991). Recently, however, a multifrequency EPR study combined with spectral simulations (Haddy et al., 1994) and a pulsed EPR study (Astashkin et al., 1994) favor an $S = {}^5/_2$ state as the more likely origin of the $g = 4.1$ signal.

Several groups have attempted to obtain information on the magnetic properties of the different S states of the Mn cluster by examining their influence on the spin−lattice relaxation characteristics of the dark-stable tyrosine radical in PSII, $Y_D^{\bullet}$. In one of the initial studies by de Groot et al. (1986), the method of inversion−recovery was used to measure the spin−lattice relaxation of $Y_D^{\bullet}$. It was observed that, in O_2-evolving PSII particles, the spin−lattice relaxation of $Y_D^{\bullet}$ was non-single-exponential and was enhanced by a species associated with the OEC. The average spin−lattice relaxation time of $Y_D^{\bullet}$ was found to decrease as the OEC was advanced to higher S states. A subsequent study by Evelo et al. (1989) used single saturating laser flashes to advance the S states. A statistical model was used to decompose the spin−lattice relaxation traces by assuming a constant amount of misses (8%) for each laser flash and no double hits. An average relaxation time was thus calculated for each S state, and it was found to be maximal in the S_1 state, minimum in the S_0 state, and intermediate in the S_2 and S_3 states. The distance between the Mn cluster and $Y_D^{\bullet}$ was estimated to be 28−43 Å from an analysis of the temperature dependence of the spin−lattice relaxation enhancement of $Y_D^{\bullet}$ by the S_0 state. However, in order to account for the non-single-exponential spin−lattice relaxation of $Y_D^{\bullet}$, it was proposed that two Mn centers are close to $Y_D^{\bullet}$ at different distances.

Beck et al. (1990) presented evidence that the non-single-exponential spin−lattice relaxation of $Y_D^{\bullet}$ was due to the powder distribution of the orientation-dependent dipolar relaxation enhancement by both the Mn cluster and the nonheme Fe^{2+}. Subsequently, Evelo and Hoff (1991) examined the possibility that the orientation dependence of the dipolar relaxation enhancement of $Y_D^{\bullet}$ causes the spin−lattice relaxation to be non-single-exponential. By assuming the distance between the Mn cluster and $Y_D^{\bullet}$ as known [$r =$ 35 Å, from Evelo et al. (1989)], they successfully simulated the spin−lattice relaxation of $Y_D^{\bullet}$ at 5 K in S_2-state PSII, yielding a correlation time of 0.14 μs for the S_2 state.

Styring and Rutherford (1988) used the continuous-wave (cw) EPR technique of progressive microwave-power saturation to examine the effect of the S states on the $P_{1/2}$ (microwave power at half-saturation) value of $Y_D^{\bullet}$. They also used saturating laser flashes to advance the S states and reached qualitatively similar conclusions as Evelo et al. (1989) concerning the potency of the different S states as relaxers of $Y_D^{\bullet}$ [$P_{1/2}(S_1) < P_{1/2}(S_2) \approx P_{1/2}(S_3) < P_{1/2}(S_0)$ at $T = 8$ K].

More recently, Kawamori and co-workers (Kodera et al., 1992, 1994) have used time-resolved EPR methods to study the spin−lattice relaxation enhancement of $Y_D^{\bullet}$ by the OEC. On the basis of the observation of a maximum of the $P_{1/2}$ value of $Y_D^{\bullet}$ at about 90 K in a sample prepared in the S_2 state, the correlation time of the S_2 state was estimated to be about 10^{-11} s. This value was used to calculate a distance of 24−27 Å between the Mn cluster and $Y_D^{\bullet}$ (Kodera et al., 1992). Later, a pulsed EPR selective hole-burning method was used to estimate a distance of 28−30 Å (Kodera et al., 1994). Un et al. (1994) have estimated this distance to be 25−35 Å from an analysis of the line shape of the $Y_D^{\bullet}$ EPR signal measured at 245 GHz.

Recently, there has been significant progress in characterizing the magnetic properties of the S_2-state multiline EPR signal species (Lorigan & Britt, 1994) and the spin−lattice relaxation of $Y_D^{\bullet}$ (Koulougliotis et al., 1992, 1995; Hirsh et al., 1992a). This presents the opportunity to analyze quantitatively the spin−lattice relaxation enhancement of $Y_D^{\bullet}$ by the S_2-state multiline EPR signal species. We have used a dipolar model (Hirsh et al., 1992a) to fit the observed saturation−recovery EPR traces for $Y_D^{\bullet}$ and to explain its non-single-exponential spin−lattice relaxation in terms of a dipole−dipole interaction with the S_2-state multiline EPR signal species. The temperature dependence of the dipolar rate constants above 4 K is explained by taking into account

the well-documented magnetic properties of the S_2-state multiline EPR signal species. A significant conclusion is that excited spin states of the S_2-state multiline EPR signal species dominate the spin−lattice relaxation enhancement of $Y_D^\bullet$ above 10 K, and this contribution has not been taken into account in past efforts to estimate the distance between the Mn cluster and $Y_D^\bullet$ from spin relaxation data. The spin−lattice relaxation enhancement of $Y_D^\bullet$ by the ground $S = {}^1/_2$ spin state of the S_2-state multiline EPR signal species has a dramatic temperature dependence below 4 K. This is interpreted to arise from ^{55}Mn nuclear spin−lattice relaxation processes which average the effective Larmor frequency of the S_2-state multiline EPR signal species and make it a better relaxation enhancer as the temperature increases from 1.8 to 4 K. Without a complete understanding of the nuclear spin relaxation processes, analysis of the spin−lattice relaxation enhancement of $Y_D^\bullet$ by the S_2 state only allows one to estimate a lower limit of 22 Å for the distance between $Y_D^\bullet$ and the Mn cluster.

MATERIALS AND METHODS

Sample Preparation. PSII membranes were prepared from market spinach leaves as described in Beck et al. (1985) and stored at 77 K in a solution containing 20 mM MES (2-(*N*-morpholino)ethanesulfonic acid)-NaOH, pH 6.0, 15 mM NaCl, 5 mM $CaCl_2$, and 30% (v/v) ethylene glycol. Samples for EPR spectroscopic studies were dark adapted for approximately 4 h in an ice−water bath followed by freezing at 77 K in complete darkness to ensure a homogeneous population of the Mn site in the diamagnetic S_1-resting state (Koulougliotis et al., 1992). All the samples also contained 300 μM DCBQ (2,5-dichloro-*p*-benzoquinone), and in some cases 100 μM DCMU [3-(3,4-dichlorophenyl)-1,1-dimethylurea], added from 20 mM stock solutions in ethanol. The method of continuous illumination (700 W/m^2) at 195 K (dry ice−ethanol bath) for 2.5 min followed by immediate freezing at 77 K was used to generate the S_2 state.

Treatment of PSII membranes with ammonia was done as in Beck et al. (1986) and included pre-equilibration of the membranes in resuspension buffer containing 20 mM Hepes (*N*-(2-hydroxyethyl)piperazine-*N*′-2-ethanesulfonic acid)-NaOH, pH 7.5, 15 mM NaCl, 5 mM $CaCl_2$, and 30% (v/v) ethylene glycol, through two resuspension and centrifugation cycles. A 1.25 M stock solution of NH_4Cl in the resuspension buffer was prepared just prior to use, and an aliquot was added (in complete darkness) to the EPR sample to give a final concentration of 100 mM NH_4Cl. The NH_4Cl-treated EPR samples, containing 300 μM DCBQ, were incubated on ice in the dark for 10−15 min after treatment before freezing at 77 K. The altered S_2-state multiline EPR signal in NH_4Cl-treated samples was produced by continuous illumination for 2.5 min at 195 K followed by dark incubation in a CCl_4 slush bath (250 K) for 6.5 min. The chlorophyll concentration in all EPR samples was 4−6 mg of Chl/mL.

Instrumentation. Saturation−recovery EPR spectroscopy was performed on a home-built X-band pulsed EPR spectrometer (Beck et al., 1991). Temperature control was achieved with either an Oxford ESR 900 (for $T > 4$ K) or an ESR 910 (for $T < 4$ K) liquid He cryostat. The temperature was determined with a Si-diode sensor at the sample position (ESR 900 cryostat) or through measurement of the He gas pressure in the secondary pumping system (ESR 910 cryostat). The magnetic field was set 6−8 G downfield from the zero-crossing point of the first-derivative X-band EPR spectrum of the $Y_D^\bullet$ radical to minimize the potential contribution from the small amount of the Chl_Z^+ radical induced by low-temperature illumination (<5%); Chl_Z is a redox-active chlorophyll that is an alternate electron donor in PSII (Thompson & Brudvig, 1988). Data acquisition and fitting of the saturation−recovery transients were performed as described earlier (Hirsh et al., 1992a; Koulougliotis et al., 1994). In particular, the scalar rate constants ($k_{1\text{scalar}}$) were determined by linear extrapolation to zero observing microwave power while the values of the dipolar rate constants ($k_{1\text{dipolar}}$) did not show any dependence on the observing microwave power, and thus $k_{1\text{dipolar}}$ was determined by averaging values obtained at several observing microwave powers. Continuous-wave progressive microwave-power saturation was performed on a Varian E-9 spectrometer.

THEORY

Saturation−Recovery EPR. In order to explain the spin−lattice relaxation behavior of $Y_D^\bullet$ in S_2-state PSII, we have extended the dipolar model of Hirsh et al. (1992a) to include the line shapes of the $Y_D^\bullet$ and S_2-state multiline EPR signals. The model of Hirsh et al. (1992a) is based on the theory of enhancement of the spin−lattice relaxation of a paramagnetic species due to dipolar interactions with neighboring paramagnets developed by Bloembergen (1949) and Abragam (1955, 1961). For a pairwise dipolar interaction between a slow- and a fast-relaxing paramagnet, there are two major contributions to the spin−lattice relaxation rate of the observed (slow) spin: (i) an isotropic term from the intrinsic relaxation rate (k_{1i}) of the species in the absence of any spin−spin interactions and (ii) an orientation-dependent term ($k_{1\theta}$) arising from the dipolar interaction between the two paramagnets.

For a nonoriented protein in a frozen solution, the orientation of the interspin vector and the applied magnetic field is random, and the angle, θ, between them can take all possible values between 0 and π. The resulting angular distribution of spin−lattice relaxation rates gives rise to non-single-exponential relaxation kinetics. For two isotropic spins, the saturation−recovery EPR transients can be fit by eq 1:

$$I(t) = 1 - N\int_0^\pi \sin\theta\,[\exp^{-(k_{1\text{scalar}}+k_{1\theta})t}]\,d\theta \qquad (1)$$

where $I(t)$ is the normalized intensity of the saturation−recovery EPR transient at time t, N is an adjustable scaling factor, $k_{1\text{scalar}}$ is the isotropic contribution to the relaxation rate, and $k_{1\theta}$ is the orientation-dependent dipolar contribution to the relaxation rate expressed by eqs 2 and 3. An exchange interaction between the two spins may produce an additional contribution to the relaxation rate, and the appropriate equations are given in Rakowsky et al. (1995). However, in the case of the interaction between $Y_D^\bullet$ and the S_2-state multiline EPR signal species, the exchange interaction is negligible owing to the large distance between the spins, resulting in $k_{1\text{scalar}} = k_{1i}$ (vide infra).

The choice of the term of the dipolar alphabet [*B*, *C*, or *E*; see Hirsh et al. (1992a) for the analytical expressions] having the largest contribution to $k_{1\theta}$ requires knowledge of the correlation time (T_{1f} or T_{2f}) dominating the relaxation

characteristics of the fast-relaxing spin as well as the Larmor frequencies (ω_s, ω_f) of the two interacting spins. Since the E-term contains the squared sum, $(\omega_s + \omega_f)^2$, of the Larmor frequencies in the denominator, it is always much smaller in magnitude than either the *B* or *C* term. In the case of the $Y_D^\bullet$ radical (slow relaxer) interacting with the S_2 state of the Mn cluster (fast relaxer), the Larmor frequencies of the two paramagnetic species are of similar magnitude. Therefore, the term $(\omega_s - \omega_f)^2$ present in the denominator of the expression for the *B* term (see eq 3) is small and makes the magnitude of the *B* term large with respect to the *C* term, which contains the term ω_s^2 in the denominator. In addition, the spin−lattice relaxation rate ($1/T_{1f}$) of the S_2-state multiline EPR signal species has been measured directly by Lorigan and Britt (1994), and it was shown to exhibit a very steep temperature dependence ($\propto T^{(8.0\pm0.4)}$) between 4.2 and 11 K. Since the *C* term of the dipolar alphabet is proportional to $1/T_{1f}$ [see Hirsh et al. (1992a) for the analytical expression], the experimentally observed dipolar rate constants should exhibit a similarly steep temperature dependence, if T_{1f} is the relevant correlation time for the relaxation enhancement of $Y_D^\bullet$ by the S_2-state multiline EPR signal species. However, the observed dipolar spin−lattice relaxation rates exhibit a much weaker ($\propto T^{1.0}$) temperature dependence (vide infra). These arguments justify the use of the *B* term over the *C* term. The analytical expression for the *B* term is given in eqs 2 and 3:

$$k_{1\theta} = k^{B}_{1dipolar}(1 - 3\cos^2\theta)^2 \tag{2}$$

where

$$k^{B}_{1dipolar} = \frac{\gamma_s^2 \mu_f^2 T_{2f}}{6r^6[1 + (\omega_s - \omega_f)^2 T_{2f}^2]} \tag{3}$$

and *r* is the interspin distance, γ_s and ω_s are the magnetogyric ratio and the Larmor frequency of the slow-relaxing spin, respectively, and μ_f and T_{2f} are the magnetic moment and the spin−spin relaxation time of the fast-relaxing spin, respectively.

Several assumptions are made in the derivation of eqs 1−3. First, it is assumed that the magnetic moments of both the fast- and slow-relaxing spins are isotropic. This is a reasonable approximation for the interaction of the S_2-state multiline EPR signal species with $Y_D^\bullet$ because, for both spins, the *g*-anisotropy is small and the inhomogeneous EPR line shapes are dominated by isotropic hyperfine splittings. Second, the Larmor frequencies of both the fast- and slow-relaxing spins are approximated as fixed, single values taken at the centroids of the respective EPR signals. This approximation neglects the fact that the two spins have a distribution of Larmor frequencies depending on the EPR line shapes. In the case of the interaction of the S_2-state multiline EPR signal species with $Y_D^\bullet$, the EPR signal from $Y_D^\bullet$ is quite narrow whereas the S_2-state multiline EPR signal extends over several thousand Gauss. Consequently, a fixed Larmor frequency approximation is not accurate, and an extension of the dipolar model of Hirsh et al. (1992a) is necessary.

If the Larmor frequency of the fast-relaxing spin remains fixed during the time scale for spin−lattice relaxation of the observed spin, the values of ω_f and ω_s for the pairwise spin−spin interaction will vary statistically throughout the ranges determined by the inhomogeneous EPR line shapes. In this case and when the magnetic moments of both spins are isotropic, eq 1 can be extended by integrating over the spectral line shapes of both EPR signals as shown in eq 4:

$$I(t) = 1 - N\int_{-\infty}^{\infty}\int_{-\infty}^{\infty}\int_{0}^{\pi} g_s(\omega_s)\, g_f(\omega_f) \sin\theta \, [\exp^{-(k_{1scalar}+k_{1\theta})t}]\, d\omega_s\, d\omega_f\, d\theta \tag{4}$$

where $g_s(\omega)$ and $g_f(\omega)$ are normalized line shape functions of the $Y_D^\bullet$ and the S_2-state multiline EPR signals, respectively, and the remaining terms are as in eq 1. Both EPR line shapes were approximated as Gaussians. Numerical simulations of saturation−recovery EPR transients were carried out by using eq 4 and programs written with Mathematica on a Sun SPARC Server 1000.

Progressive Microwave-Power Saturation. The effect of progressive microwave-power saturation on an inhomogeneously broadened resonance has been described by Portis (1953), Castner (1959), and Beinert and Orme-Johnson (1967). The empirical equation usually used to express the EPR derivative-signal amplitude (**S**) is the following (Rupp et al., 1978):

$$\mathbf{S} = \frac{k\sqrt{P}}{(1 + P/P_{1/2})^{b/2}} \tag{5}$$

where *b* is the inhomogeneity parameter varying between $b = 1$ (completely inhomogeneous line broadening) and $b = 3$ (completely homogeneous line broadening), *k* is a proportionality factor, *P* is the applied microwave power, and $P_{1/2}$ is the microwave power at half-saturation. $P_{1/2}$ is proportional to $(\mathbf{H}_{1/2})^2$, the microwave field needed to saturate a spin packet, and defined by $(\mathbf{H}_{1/2})^2 = 1/(\gamma^2 T_1 T_2)$. Thus, $P_{1/2}$ provides a measure of the relaxation characteristics of the observed species, even though the temperature dependence obtained cannot discriminate between T_1 and T_2 effects.

Microwave-power saturation studies have been done on the S_2-state multiline EPR signal in order to identify the relaxation mechanism applicable to the signal (de Paula & Brudvig, 1985; Pace et al., 1991). At temperatures above about 2 K, the two common relaxation mechanisms observed are the Raman and the Orbach processes. The Raman process proceeds through a "virtual" excited state by the absorption and emission of two phonons whose energy difference matches the one between the electron spin states (Van Vleck, 1940). The entire phonon spectrum can contribute to Raman relaxation. The Raman relaxation rate, $1/T_1$, exhibits a T^n temperature dependence with the value of *n* typically ranging between 3 and 9. If, however, a real low-lying excited-state spin manifold exists above the ground-state manifold, the Orbach process (Orbach, 1961a,b) can dominate the relaxation pathway. In the Orbach process, only phonons with an energy $h\nu \approx \Delta$ contribute to the relaxation mechanism, where Δ is the energy difference between the ground and excited spin states. As a result, the temperature dependence is different; in the low-temperature limit ($kT \ll \Delta$), the Orbach relaxation rate, $1/T_1$, is proportional to $\exp(-\Delta/kT)$. If an Orbach relaxation mechanism can be shown to apply, then the energy difference, Δ, can be determined.

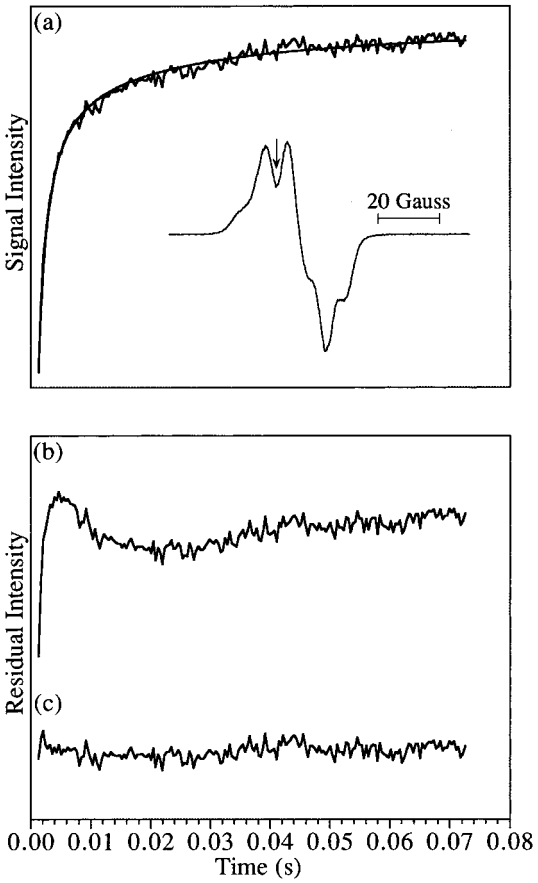

FIGURE 1: (a) Saturation−recovery EPR transient obtained for $Y_D^•$ in untreated PSII membranes with the Mn cluster poised in the S_2-state multiline EPR signal form. The transient was obtained at 6.8 K, and the fit, obtained by using the *B* term of the dipolar model (eqs 1−3), is shown superimposed. The observing microwave power was 0.58 μW, the saturating microwave pulse power was 72 mW, and the pulse was of 12 ms duration. The residuals (difference between the saturation−recovery EPR transient and the fitted curve) are shown for (b) the single-exponential fit and (c) the dipolar-model fit. Inset: First-derivative cw X-band EPR spectrum centered at $g = 2.0$ measured with the following experimental conditions: temperature, 5.6 K; microwave frequency, 9.07 GHz; field-modulation amplitude, 4 G; microwave power, 0.72 μW; field-modulation frequency, 100 kHz. The arrow indicates the magnetic field used for the saturation−recovery EPR experiments.

RESULTS

Relaxation Enhancement of $Y_D^•$ by the S_2-State Multiline EPR Signal Species. Saturation−recovery EPR spectroscopy was performed on $Y_D^•$ in samples prepared in the $S_2 - Q_A^-$ state by 200 K illumination. The cw EPR spectrum of $Y_D^•$ is shown in the inset of Figure 1a. A typical saturation−recovery EPR transient obtained for $Y_D^•$ is shown in Figure 1a with the dipolar-model fit (eqs 1−3) superimposed. The transient is non-single-exponential as evidenced from the residual for a single-exponential fit (Figure 1b). This behavior persisted over the entire temperature range examined (1.8 K < T < 55 K).

The dipolar ($k^B_{1dipolar}$) and the scalar ($k^B_{1scalar}$) rate constants for $Y_D^•$ in S_2-state PSII are plotted as a function of temperature in Figure 2a. These data can be compared to the solid lines in Figure 2a which are linear least-squares fits to the dipolar and scalar rate constants obtained for $Y_D^•$ in Mn-depleted PSII [data from Hirsh et al. (1992a)]. The values of $k^B_{1scalar}$ from Mn-depleted PSII are identical,

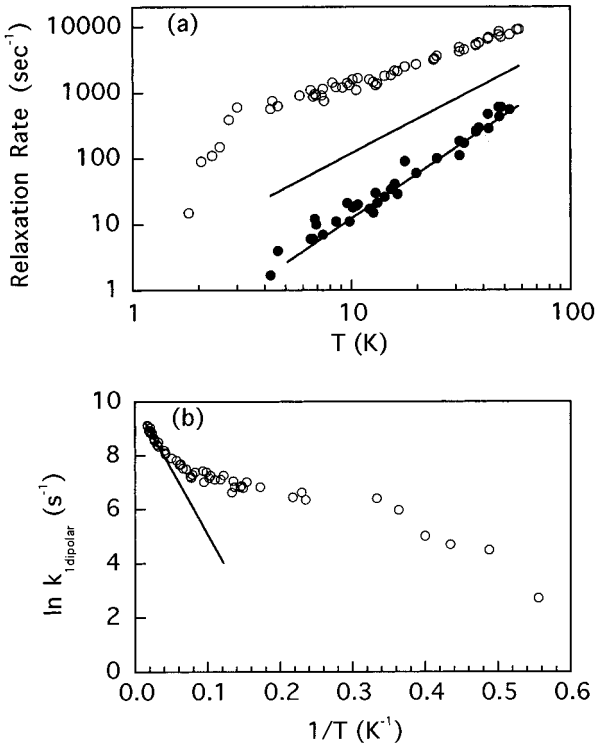

FIGURE 2: (a) Temperature dependence of the scalar [$k^B_{1scalar}$ (●)] and dipolar [$k^B_{1dipolar}$ (○)] rate constants obtained from fits of eqs 1−3 to data from $Y_D^•$ in untreated PSII membranes with the Mn cluster poised in the S_2-state multiline EPR signal form. The lines through the filled circles and between the two sets of data points are linear least-squares fits to the scalar ($k^B_{1scalar}$) and dipolar ($k^B_{1dipolar}$) rate constants, respectively, for $Y_D^•$ in Mn-depleted PSII [data from Hirsh et al. (1992a)]. (b) Plot of the natural log vs 1/T of the $k^B_{1dipolar}$ values from panel a for $Y_D^•$ in untreated PSII membranes with the Mn cluster poised in the S_2-state multiline EPR signal form. The solid line represents a linear least-squares fit of the experimental data taken at temperatures above 30 K yielding a slope of −48.4 K, corresponding to an energy difference (Δ) of 34 cm^{-1} between the ground and first excited spin-state manifolds.

within experimental error, to the ones obtained for $Y_D^•$ in S_2-state PSII. This excellent agreement supports the use of the dipolar model to analyze the data. The values of $k^B_{1scalar}$ are also identical to the intrinsic relaxation rate constants (k_{1i}) measured directly for $Y_D^•$ in the CN^- derivative of Mn-depleted PSII (Koulougliotis et al., 1995). These results indicate that there exists no contribution to the relaxation of $Y_D^•$ from exchange coupling due to spatial orbital overlap between the Mn cluster and $Y_D^•$.

In addition to the S_2 state, the high-spin nonheme Fe^{2+} ($S = 2$) of the electron-acceptor side also acts as a relaxation enhancer of $Y_D^•$. Its effect has been characterized through measurements in Mn-depleted PSII membranes, in which the nonheme Fe^{2+} acts as the sole relaxation enhancer of $Y_D^•$ (Hirsh et al., 1992a; Koulougliotis et al., 1995). A comparison of the magnitude of the values of $k^B_{1dipolar}$ of $Y_D^•$ in Mn-depleted and in S_2-state PSII (Figure 2a, upper solid line and open circles, respectively) shows that the relaxation enhancement by the S_2 state is much greater than that by the nonheme Fe^{2+}. We conclude that the contribution of the nonheme Fe^{2+} to the relaxation enhancement of $Y_D^•$ is insignificant, relative to that of the S_2 state, over the temperature range studied. The same conclusion was reached by Bosch et al. (1991) based on a consideration of the flash-

induced oscillation of the spin−lattice relaxation enhancement of $Y_D^{\bullet}$.

The dipolar relaxation enhancement of $Y_D^{\bullet}$ by the S_2 state multiline EPR signal species shows a weak temperature dependence above 3 K but decreases dramatically below 3 K. We will first consider the temperature dependence of $k^B_{1dipolar}$ above 3 K and then consider the lower temperature data. In order to explain the origin of the temperature dependence of the dipolar relaxation enhancement, we need to examine which terms in the theoretical expression for $k^B_{1dipolar}$ could change with temperature. As seen in eq 3, two terms could be a function of temperature: the magnetic moment, μ_f^2, and the transverse relaxation time, T_{2f}, of the fast-relaxing spin. T_{2f} is normally considered to be independent of temperature for spins trapped in a rigid lattice. However, since the relation $T_{1f} \geq T_{2f}$ has to hold, T_{2f} will follow the same temperature dependence as T_{1f} when the latter is smaller. T_{1f} and $k^B_{1dipolar}$ exhibit dramatically different temperature dependencies above 3 K: approximately $T^{8.0}$ (Lorigan & Britt, 1994) and approximately $T^{1.0}$ (this work), respectively. This indicates that a temperature dependence of T_{2f} is not the origin of the observed temperature variation of $k^B_{1dipolar}$ above 3 K.

Previously, we examined the spin−lattice relaxation enhancement of a stable phenoxyl radical by a neighboring diferric cluster in two different systems: the R2 subunit of ribonucleotide reductase (Hirsh et al., 1992b; Galli et al., 1994) and a model compound (Goldberg et al., 1995). In these studies, it was shown that the change in μ_f^2 of the diferric cluster, due to population of its first excited spin state as the temperature rises, completely accounted for the temperature dependence of the dipolar-induced spin−lattice relaxation enhancement of the radical. As a result, a plot of $\ln(k^B_{1dipolar})$ versus $1/T$ is linear with a slope proportional to the energy separation, Δ, between the ground and first excited spin states. An analogous plot of the dipolar rate constants obtained for $Y_D^{\bullet}$ in S_2-state PSII is shown in Figure 2b. The limiting slope at high temperature corresponds to an energy separation between the ground and first excited spin states of 34 cm^{-1}. This is in good agreement with the energy difference of 36.5 cm^{-1} between the ground ($S = {}^1/_2$) and the first excited spin state of the S_2-state multiline EPR signal species determined by Lorigan and Britt (1994).

These results provide a strong indication that the temperature dependence above 3 K of $k^B_{1dipolar}$ for $Y_D^{\bullet}$ in S_2-state PSII can be explained quantitatively by taking into account the already known magnetic properties of the S_2 state. As the temperature is raised, the population of the first excited spin state changes the magnitude of μ_f^2 according to the following equation:

$$\mu_f^{\,2} = g_f^{\,2}\beta^2 \frac{1.5 + S(S+1)(2S+1)e^{-\Delta/kT}}{2 + (2S+1)e^{-\Delta/kT}} \qquad (6)$$

In eq 6, the energy of the ground state is taken to be zero, the spin of the ground state is ${}^1/_2$, and the spin of the first excited state is denoted as S. By taking into account the known value for $\Delta = 36.5$ cm^{-1} and collecting terms, we can substitute the expression for μ_f^2 (eq 6) into eq 3, which thus takes the following form:

$$k^B_{1dipolar} = \frac{m1 + m2e^{-52/T}}{2 + (2S+1)e^{-52/T}} \qquad (7)$$

where T is in units of cm^{-1}, and $m1$ and $m2$ are constants that depend on the properties of the two spins and the interspin distance (see eq 3). The contributions of the ground spin state ($S = {}^1/_2$) and the first excited spin state of the S_2-state multiline EPR signal species to the spin−lattice relaxation enhancement of $Y_D^{\bullet}$ are given by $m1/(2 + (2S + 1)e^{-52/T})$ and $m2e^{-52/T}/(2 + (2S + 1)e^{-52/T})$, respectively. We have fit the values of $k^B_{1dipolar}$ shown in Figure 2 for 3 K < T < 80 K by using eq 7 with different values for the spin multiplicity S of the first excited spin state (${}^1/_2 < S < 11/2$) and observed that the fits are satisfactory for $S < {}^7/_2$ (Koulougliotis, 1995). We conclude that the temperature dependence of $k^B_{1dipolar}$ at temperatures above 3 K is accurately accounted for by the change of μ_f^2.

The ground $S = {}^1/_2$ spin state of the S_2-state multiline EPR signal species provides the dominant contribution to the spin−lattice relaxation enhancement of $Y_D^{\bullet}$ below 10 K. Over this temperature range, the two temperature-dependent terms in eq 3, μ_f^2 and T_{2f}, are constant, and it would be expected that the spin−lattice relaxation enhancement of $Y_D^{\bullet}$ below 10 K would also be constant. Indeed, the spin−lattice relaxation enhancement of $Y_D^{\bullet}$ approaches an asymptotic value of about 830 s^{-1} over the 3−10 K range (Figure 2). Previous studies have used a single, fixed Larmor frequency model (eqs 1−3) to estimate the distance between $Y_D^{\bullet}$ and the Mn cluster from spin relaxation enhancement data. Before including the EPR line shapes or considering the dramatic decrease below 3 K in the effectiveness of the S_2-state multiline EPR signal species for spin relaxation enhancement of $Y_D^{\bullet}$, we first consider the use of eqs 1−3 to estimate the distance between $Y_D^{\bullet}$ and the Mn cluster from the spin relaxation enhancement data in the 3−10 K range.

The values of all of the terms in eq 3 are known except the value of T_{2f}. A lower limit to T_{2f} can be set by measurement of the phase-memory time, T_M, through an electron spin-echo experiment. Fitting the two-pulse spin-echo decay obtained for the S_2-state multiline EPR signal by Britt et al. (1989) as well as by Zimmermann et al. (1993) to a single exponential gives $T_M \approx 0.8$ μs at 4.2 K. 0.8 μs is a lower limit to T_{2f}, since the two-pulse spin-echo decay of the S_2-state multiline EPR signal may have contributions from spectral-diffusion processes. However, numerous similar spin-echo decay measurements for either isolated nitroxyl radicals or for metal centers have, in all cases, given values for T_M close to the one measured for the S_2-state multiline EPR signal (i.e., a few hundred nanoseconds) over a very wide temperature range (4−40 K) [see for example Nakagawa et al. (1992) and Rakowsky et al. (1995)]. The values for T_M have also given reasonable estimates of T_2 based on the single-exponential nature of the spin-echo decay (Nakagawa et al., 1992), which is also observed for the S_2-state multiline EPR signal, and on successful theoretical simulation of relaxation-enhancement data (Rakowsky et al., 1995). Thus, we conclude that 0.8 μs is a reasonable estimate of the value of T_{2f} of the S_2-state multiline EPR signal species. The remaining terms in eq 3 have the following values: $\nu_s = \omega_s/2\pi = 9.07$ GHz, $g_s = 2.0046$ (Miller & Brudvig, 1991), $\gamma_s^2 = 4\pi^2 g_s^2 \beta^2/h^2$, and $g_f = 1.982$ (Hansson et al., 1987); a recent multifrequency study of the

S_2-state multiline EPR signal found $g_f = 1.975-1.985$ (Åhrling & Pace, 1995). With these values and the asymptotic dipolar relaxation rate of 830 ± 180 s^{-1} over the temperature range 3−10 K, the distance between Y_D and the Mn cluster is calculated to be 19 ± 1 Å by using eq 3. This distance is unreasonably short in light of computer models of the D1/D2 complex based on the structure of the bacterial reaction center (see Discussion). Moreover, this analysis does not take into account the line shapes of the $Y_D^\bullet$ and S_2-state multiline EPR signals nor does it explain the dramatic decrease below 3 K in the effectiveness of the S_2-state multiline EPR signal species for spin relaxation enhancement of $Y_D^\bullet$.

To address the effect of the EPR line shapes, numerical simulations of saturation−recovery EPR data for $Y_D^\bullet$ were done by using eq 4. Equation 4 includes the EPR line shapes in the limit when the Larmor frequency of the S_2-state multiline EPR signal species remains fixed during the spin−lattice relaxation time of $Y_D^\bullet$. In this limit, as the line width of the fast-relaxing spin increases, its effectiveness as a relaxation enhancer decreases (Figure 3, inset) because more of the pairwise interactions involve large values of $\Delta\omega^2 = (\omega_s - \omega_f)^2$. The half-width at half-height of the S_2-state multiline EPR signal is about 250 gauss, and that of $Y_D^\bullet$ is about 11 gauss. With a 250-gauss line width for the S_2-state multiline EPR signal, it was found that including a 11-gauss line width for the $Y_D^\bullet$ EPR signal gave the same result as a fixed Larmor frequency for $Y_D^\bullet$. Also, small variations in the *g*-value of the S_2-state multiline EPR signal over the range 1.975−1.985 found by Åhrling and Pace (1995) had no effect. A numerical simulation using eq 4 of spin−lattice relaxation data taken at 6.8 K is shown in Figure 3a; the best-fit distance between Y_D and the Mn cluster is 13 Å, which is even shorter than the value of 19 Å calculated by using eqs 1−3. Clearly, including the line shapes in this way still yields an unreasonably short estimate for the distance between Y_D and the Mn cluster. Moreover, the above analysis does not account for the decrease below 3 K in the effectiveness of the S_2-state multiline EPR signal species for spin relaxation enhancement of $Y_D^\bullet$. In order to explain these results, we present the following new dynamic model for relaxation enhancement of $Y_D^\bullet$ by the S_2-state multiline EPR signal species.

The dipolar interaction between $Y_D^\bullet$ and the S_2-state multiline EPR signal species is a rather unusual case because the large inhomogeneous line width of the S_2-state multiline EPR signal is due to large isotropic ^{55}Mn nuclear hyperfine interactions. Typically, a large EPR line width is the result of anisotropy in the *g*-value or zero-field splitting interaction. In these latter cases, a saturation−recovery EPR measurement at a specific magnetic field would select a fixed set of Larmor frequencies of the fast-relaxing spins; ω_f of a given spin could not change significantly in a solid-state sample because it is fixed by the rigid orientation. A well-known example is orientation selection in ENDOR measurements of proteins in frozen solutions (DeRose & Hoffman, 1995). In contrast, ^{55}Mn nuclear spin−lattice relaxation could greatly modulate the effective Larmor frequency of the S_2-state multiline EPR signal species, if it occurs on the same time scale as the spin−lattice relaxation of $Y_D^\bullet$. Indeed, nuclear spin transitions are known to occur within the time scale for spin−lattice relaxation of $Y_D^\bullet$. For example, nuclear spin transitions are responsible for spectral diffusion during saturation−recovery EPR measurements of isolated paramagnets (Beck et al., 1991) and also are the basis of the technique of pulse field-sweep EPR (Falkowski et al., 1986). As a result of nuclear spin transitions, the Larmor frequency of the S_2-state multiline EPR signal species could change during the time scale of spin−lattice relaxation of $Y_D^\bullet$. Such averaging of the Larmor frequency of the S_2-state multiline EPR signal species would cause the effective value of $\Delta\omega^2 = (\omega_s - \omega_f)^2$ to be decreased, which would make the S_2-state multiline EPR signal species a more effective relaxation enhancer owing to the fact that the relaxation enhancement increases dramatically when $\Delta\omega^2$ is close to zero (eq 3). The dramatic decrease in effectiveness of the S_2-state multiline EPR signal species as a relaxation enhancer of $Y_D^\bullet$ below 3 K can be explained by this model. In this case, ^{55}Mn nuclear

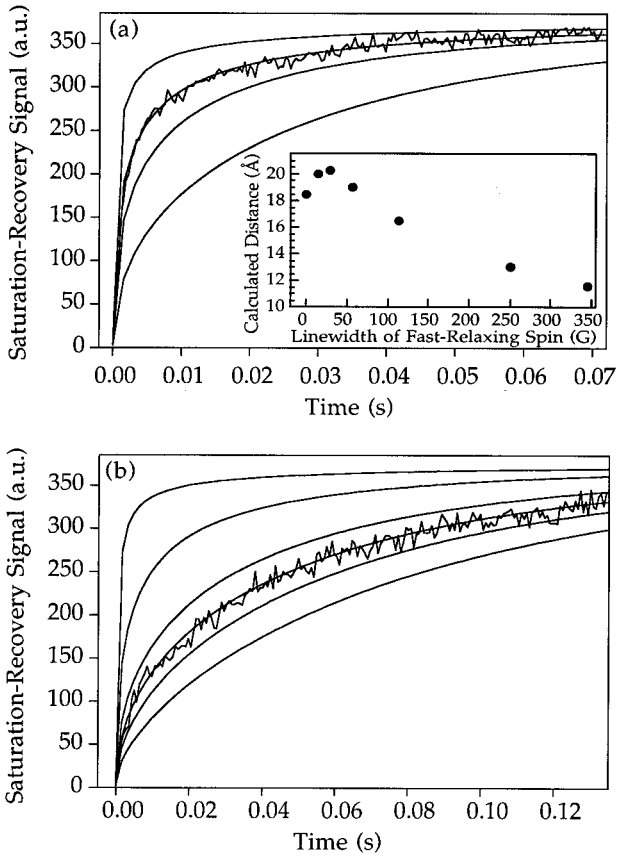

FIGURE 3: (a) Comparison of an experimental saturation−recovery EPR transient of $Y_D^\bullet$ taken at 6.8 K (same data as in Figure 1a) with a series of simulated recoveries calculated with eq 4. The different simulated curves were calculated by varying the distance between the fast- and slow-relaxing spins ($r = 10$, 13, 15, and 20 Å, from top to bottom, respectively), and the remaining parameters were fixed at the following values: line width and *g*-value of the S_2-state multiline EPR signal, 250 G and 1.982, respectively; line width and *g*-value of the $Y_D^\bullet$ EPR signal, 11 G and 2.0046, respectively; $T_{2f} = 0.8$ μs; and $k_{1scalar} = 14$ s^{-1}. Inset: Plot of the best-fit value of *r* from simulations using eq 4 of the experimental saturation−recovery EPR transient of $Y_D^\bullet$ shown in Figure 3a vs the line width of the fast-relaxing spin; all of the remaining parameters were as in Figure 3a. (b) Comparison of an experimental saturation−recovery EPR transient of $Y_D^\bullet$ taken at 1.8 K with a series of simulated recoveries calculated by using eq 4. The experimental data were obtained with an observing microwave power of 72 nW, a saturating microwave pulse power of 180 mW, and a pulse duration of 20 ms. The different simulated curves were calculated by varying the distance between the fast- and slow-relaxing spins ($r = 10$, 15, 20, 22.5, 25, and 30 Å, from top to bottom, respectively), and the remaining parameters were as in Figure 3a except $k_{1scalar} = 8$ s^{-1}.

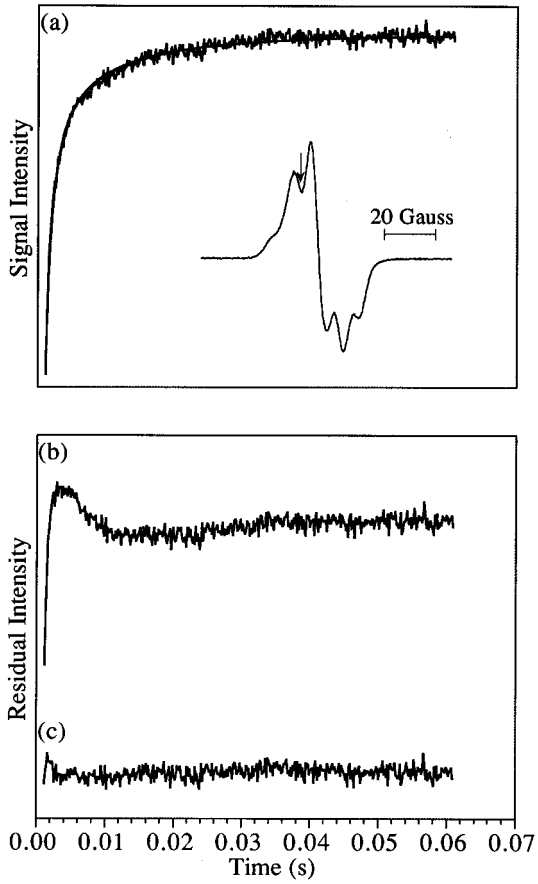

FIGURE 4: (a) Saturation−recovery EPR transient obtained for $Y_D^\bullet$ in NH_3-treated PSII membranes where the Mn cluster is poised in the altered S_2-state multiline EPR signal form. The transient was obtained at 7.5 K and the fit, obtained by using the *B* term of the dipolar model (eqs 1−3), is shown superimposed. The observing microwave power was 1.44 μW, the saturating microwave pulse power was 180 mW, and the pulse was of 10 ms duration. The residuals (difference between the saturation−recovery EPR transient and the fitted curve) are shown for (b) the single-exponential fit and (c) the dipolar-model fit. Inset: First-derivative cw X-band EPR spectrum centered at $g = 2.0$ measured with the same experimental conditions as the ones given for the inset of Figure 1. The arrow indicates the magnetic field setting for the saturation−recovery experiment.

spin−lattice relaxation of the S_2-state multiline EPR signal species would be sufficiently rapid above 3 K to average ω_f, enhancing its effectiveness for relaxation enhancement, whereas at lower temperature the nuclear spin−lattice relaxation would become too slow for effective averaging of ω_f.

At sufficiently low temperature, when the nuclear spin−lattice relaxation is too slow for effective averaging of ω_f, a fixed Larmor frequency model (eq 4) will be justified to estimate the distance between $Y_D^\bullet$ and the Mn cluster. Although this low-temperature limit may not have been reached at the lowest temperature of our measurements, we can use the data taken at 1.8 K to obtain a lower limit of the distance between Y_D and the Mn cluster. A further reason that the 1.8 K data will only provide a lower limit on the distance is that the relaxation enhancement from the S_2-state may be overestimated because the contribution of the nonheme Fe^{2+} is approaching that of the S_2-state at very low temperature (Figure 2a). The best-fit distance is 22 Å for the data taken at 1.8 K (Figure 3b). From these results, a conservative estimate of the lower limit of the distance between Y_D and the Mn cluster is 22 Å.

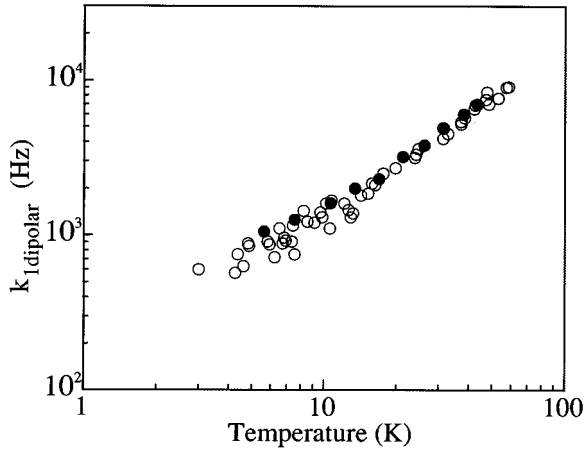

FIGURE 5: Temperature dependence of $k^B_{1dipolar}$ for the following: $Y_D^\bullet$ in NH_3-treated PSII membranes with the Mn cluster poised in the altered S_2-state multiline EPR signal form (●) and of $Y_D^\bullet$ in untreated PSII membranes with the Mn cluster poised in the S_2-state multiline EPR signal form (○).

Relaxation Enhancement of $Y_D^\bullet$ by the Altered S_2-State Multiline EPR Signal Species in NH_3-Treated Photosystem II. The inset in Figure 6 shows the altered S_2-state multiline EPR signal induced in NH_3-treated PSII membranes which is characterized by a smaller hyperfine splitting (67 ± 7 G) relative to the S_2-state multiline EPR signal observed in untreated PSII membranes (87 ± 8 G). A typical saturation−recovery EPR transient obtained for $Y_D^\bullet$ in PSII membranes prepared in the altered S_2 state is shown in Figure 4a with the dipolar-model *B*-term fit (eqs 1−3) superimposed. The cw EPR signal of the observed species, i.e., the $Y_D^\bullet$ radical, is shown in the inset. The non-single-exponential spin−lattice relaxation kinetics for the experimental transient is evidenced by the residuals from a single-exponential fit (Figure 4b).

The dipolar rate constants, $k^B_{1dipolar}$'s, extracted from the fits of eq 1 to the experimental saturation−recovery traces are plotted in Figure 5 as a function of temperature. They are superimposable, within experimental error, with the ones obtained in untreated samples containing the S_2-state multiline EPR signal. This indicates that the relaxation characteristics of the Mn cluster in the altered S_2-state multiline form are not significantly different from the ones in the "normal" S_2-state multiline form.

The complementary technique of progressive microwave-power saturation was also employed in order to assess the spin-relaxation properties of the altered S_2-state multiline EPR signal species. Figure 6 shows the power-saturation curves obtained for the altered S_2-state multiline EPR signal as a function of temperature (4.4 K < T < 10.5 K). The solid lines superimposed on the data are theoretical fits by using eq 5, where the value of b was set to 1 (inhomogeneous limit). The values for the microwave power at half-saturation, $P_{1/2}$, extracted from these fits are shown in Figure 7.

As described in the Theory section, if a species relaxes via an Orbach mechanism, its spin−lattice relaxation rate, $1/T_1$, is proportional to $e^{-\Delta/kT}$. Consequently, a plot of ln$(1/T_1)$ vs $1/T$ should be linear with a slope of $-\Delta/k$. Since $P_{1/2}$ is proportional to $1/T_1T_2$, a plot of ln$(P_{1/2})$ vs $1/T$ should also be linear if T_2 is independent of temperature over the regime employed. The linear fit superimposed on the data of Figure 7 gives a slope of −44 ± 3 K, translating to $\Delta =$

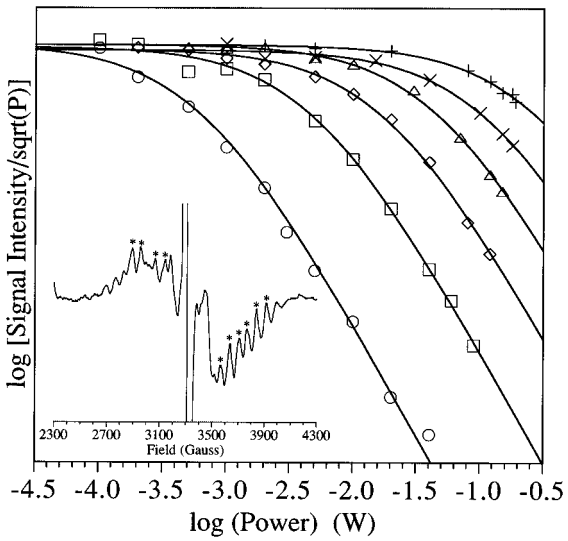

FIGURE 6: Progressive microwave-power saturation of the altered S_2-state multiline EPR signal observed in NH_3-treated PSII membranes as a function of temperature. The theoretical fits to the experimental data were done by using eq 5 for $b = 1$ in order to extract the values of $P_{1/2}$. The temperatures employed are the following: 4.4 K (○), 5.2 K (□), 6.1 K (◇), 7.2 K (△) 9.0 K (×), 10.5 K (+). Inset: Altered S_2-state multiline EPR signal induced in NH_3-treated PSII membranes. Experimental conditions were the following: temperature, 9 K; microwave frequency, 9.2 GHz; field-modulation amplitude, 20 G; microwave power, 5 mW; field-modulation frequency, 100 kHz. The average value of the height of the peaks denoted with asterisks was used as the signal intensity, **S**, in order to generate the saturation curves.

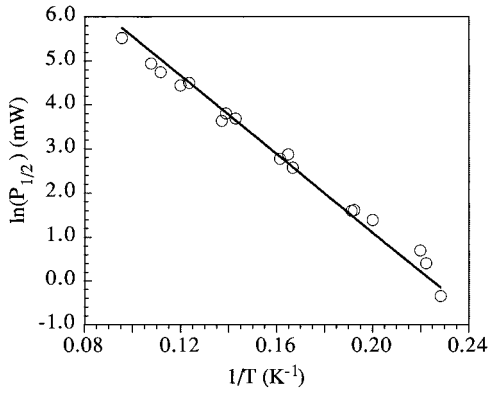

FIGURE 7: Orbach plot displaying the natural log of the microwave power at half-saturation, $P_{1/2}$, of the altered S_2-state multiline EPR signal as a function of inverse temperature. The solid line represents a linear least-squares fit of the experimental data with a slope of -44 ± 3 K, corresponding to an energy difference (Δ) of 30.5 ± 2.1 cm^{-1} between the ground and first excited spin-state manifolds.

30.5 ± 2.1 cm^{-1}. Thus, we conclude that, as in the case of the S_2-state multiline EPR signal, the altered S_2-state multiline EPR signal in NH_3-treated PSII membranes relaxes via an Orbach mechanism. The value of $\Delta = 30.5 \pm 2.1$ cm^{-1} determined for the energy difference between the ground and first excited spin state is slightly lower than the one determined from T_1 measurements of the S_2-state multiline EPR signal [$\Delta = 36.5 \pm 0.7$ cm^{-1}; Lorigan & Britt (1994)]. This could indicate a slight difference between the two forms of the signal. It is, however, important to note that the original estimation of the energy difference, Δ, for the S_2-state multiline EPR signal species in untreated PSII membranes by means of $P_{1/2}$ measurements yielded a value of $\Delta \approx 30$ cm^{-1} (Hansson et al., 1984). Thus, by combining the results of the $P_{1/2}$ measurements with those from the saturation−recovery EPR studies, we conclude that the magnetic properties of the two forms of the S_2 state of the Mn cluster are very similar, despite the considerable difference in the nuclear-hyperfine splitting exhibited in their cw EPR spectra.

DISCUSSION

In this paper, we have used saturation−recovery EPR spectroscopy to study the spin−lattice relaxation behavior of the $Y_D^\bullet$ radical in PSII membranes where the Mn cluster of the OEC was poised in the S_2 state. There exist several forms of the S_2 state. Here, we have concentrated on the two forms giving the S_2-state multiline EPR signal and the altered S_2-state multiline EPR signal in untreated and NH_3-treated PSII membranes, respectively. By using low-temperature photochemistry to limit the PSII reaction center to a single electron-transfer event, the S_2 state of the Mn cluster was produced in high yield, thus avoiding the scrambling of the S states due to misses and/or double hits present in single laser-flash experiments.

Past studies performed in Mn-depleted PSII membranes showed that the spin−lattice relaxation kinetics of $Y_D^\bullet$ are enhanced by the nonheme Fe^{2+} via a pairwise dipole−dipole interaction (Hirsh et al., 1992a; Koulougliotis et al., 1995). In the studies performed here, it was found that both forms of the S_2-state multiline EPR signal examined provide a 4−20-fold more efficient spin−lattice relaxation pathway for $Y_D^\bullet$ relative to the one provided by the nonheme Fe^{2+} [see also Bosch et al. (1991)]. This allowed the relaxation enhancement of $Y_D^\bullet$ by the S_2 state to be treated as a pairwise dipolar interaction between a slow- and a fast-relaxing species ($Y_D^\bullet$ and the S_2 state, respectively).

The temperature dependence of the dipole−dipole induced spin−lattice relaxation enhancement of $Y_D^\bullet$ above 3 K is explained by the temperature-dependent variation of the magnetic moment of the S_2-state multiline EPR signal species due to population of its first excited spin state [located 36.5 cm^{-1} higher in energy; Lorigan & Britt (1994)]. Our results show that different spin states of the S_2 state of the Mn cluster are responsible for the relaxation enhancement of $Y_D^\bullet$, depending on the temperature regime: for $T \leq 10$ K, the ground ($S = {}^1/_2$) spin state predominates, for $T \geq 30$ K it is the first excited spin state, and at intermediate temperatures the contributions of the two spin states are comparable. This picture is consistent with a single tetranuclear Mn complex acting as the relaxation enhancer of $Y_D^\bullet$, and we do not need to invoke any additional complexity in order to fit the experimental data.

In the past, variations of the spin−lattice relaxation enhancement of $Y_D^\bullet$ by the Mn cluster have been taken to be diagnostic of redox changes of the Mn cluster (de Groot et al., 1986; Boussac & Rutherford, 1994). However, our work shows that population of low-lying excited spin states of the Mn cluster contributes significantly to the relaxation enhancement of $Y_D^\bullet$ and has to be taken into account in the interpretation of the experimental data. A structural change of the Mn complex that affects the exchange couplings between the Mn ions could produce a large change in the spin−lattice relaxation enhancement of $Y_D^\bullet$ without a redox change. This is supported by past studies (Koulougliotis et al., 1992) in which it was shown that, even though it remains

in the S_1 state, the Mn cluster exhibits dramatically different spin−lattice relaxation-enhancement characteristics in short-term (active state) vs long-term (resting state) dark-adapted samples due to a structural rearrangement affecting its magnetic properties. Therefore, measurements of relaxation enhancement effects on $Y_D^{\bullet}$ cannot be used in a simple way to ascertain whether or not a redox change of Mn has occurred.

The technique of microwave-power saturation has been employed in the past to study the influence of the S_2 state on the spin−lattice relaxation of $Y_D^{\bullet}$ as a function of temperature (Styring & Rutherford, 1988; Innes & Brudvig, 1989; Kodera et al., 1992). The $P_{1/2}$ values obtained for $Y_D^{\bullet}$ in samples given one flash (Mn cluster in the S_2 state) were approximately 10-fold higher than the ones obtained in Tris-washed (i.e., Mn-depleted) PSII membranes for temperatures between 10 and 40 K. This is qualitatively in agreement with our results and provides additional support to the assumption made throughout that the nonheme Fe^{2+} is a much less efficient relaxation enhancer of $Y_D^{\bullet}$ relative to the S_2-state multiline form of the Mn cluster. A significant conclusion also deduced from the $P_{1/2}$ measurements, which is also in agreement with our work, is that $Y_D^{\bullet}$ and the Mn cluster interact magnetically. However, as discussed in Hirsh et al. (1992a) and Galli et al. (1996), the quantitative analysis of $P_{1/2}$ measurements is not straightforward when the observed species experiences a large dipolar interaction with a neighboring paramagnet. In particular, the unusual temperature dependencies of the $P_{1/2}$ values obtained for $Y_D^{\bullet}$ in O_2-evolving PSII membrane samples (Styring & Rutherford, 1988; Innes & Brudvig, 1989; Kodera et al., 1992) are probably an artifactual result of distortions of the microwave-power saturation curves caused by the dipolar interaction of $Y_D^{\bullet}$ with the Mn cluster (Galli et al., 1996).

Below 10 K, the ground $S = {}^1/_2$ spin state of the S_2-state multiline EPR signal species dominates the spin−lattice relaxation enhancement of $Y_D^{\bullet}$. In principle, because the magnetic properties of the S_2-state multiline EPR signal species are well-characterized, the low-temperature relaxation data can be quantitatively analyzed to calculate the distance between $Y_D^{\bullet}$ and the Mn cluster. However, the marked decrease below 3 K in the effectiveness of the S_2-state multiline EPR signal species for relaxation enhancement requires the contribution of an additional dynamic process. We present a new dynamic model that includes averaging of the effective Larmor frequency of the S_2-state multiline EPR signal species by ^{55}Mn nuclear spin−lattice relaxation. This is a consequence of the unusual characteristic that the S_2-state multiline EPR signal has a large inhomogeneous line width from isotropic ^{55}Mn nuclear hyperfine splittings. In order to calculate the distance between Y_D and the Mn cluster from the relaxation enhancement of $Y_D^{\bullet}$ by the S_2-state multiline EPR signal species, detailed knowledge about how ω_f changes within the time scale of the spin−lattice relaxation of the observed spin would be required. Without a detailed understanding of the ^{55}Mn nuclear relaxation processes, we can only place a lower limit on the distance between $Y_D^{\bullet}$ and the Mn cluster of 22 Å.

Our lower limit of the distance between $Y_D^{\bullet}$ and the Mn cluster is consistent with previous estimates that have been made on the basis of analyses of spin−lattice relaxation enhancements of $Y_D^{\bullet}$ by the Mn cluster. However, none of the past studies have taken into account ^{55}Mn nuclear spin−lattice relaxation effects or the significant effect of excited states of the Mn cluster on the spin−lattice relaxation enhancement of $Y_D^{\bullet}$ at $T > 10$ K. By attributing all of the relaxation enhancement at $T > 10$ K to the ground $S = {}^1/_2$ spin state of the S_2-state multiline EPR signal species, the distance will be underestimated. For example, Kodera et al. (1992) used spin−lattice relaxation data taken at 90 K to estimate a distance of 24−27 Å between $Y_D^{\bullet}$ and the Mn cluster. Other distance estimates have been made without full characterization of the magnetic properties of the Mn complex. For example, in an early study, Evelo et al. (1989) estimated a distance of 28−43 Å on the basis of the temperature dependence of the relaxation of $Y_D^{\bullet}$ in the S_0 state to determine the correlation time of the Mn cluster. However, the non-single-exponential spin−lattice relaxation kinetics of $Y_D^{\bullet}$ were interpreted in terms of two different Mn centers close to $Y_D^{\bullet}$ at different distances; this picture is not in agreement with current views. Moreover, the magnetic properties of the S_0 state were, and still are, poorly characterized. Evelo and Hoff (1991) explained the non-single-exponential spin−lattice relaxation kinetics of $Y_D^{\bullet}$ in terms of a dipolar interaction with the S_2 state of the Mn cluster. However, the internuclear distance was considered to be known ($r = 35$ Å) in order to simulate the data which, thus, yielded $\tau_c = 0.14$ μs as the relevant correlation time at $T = 5$ K. This correlation time was assigned to the spin−lattice relaxation time of the Mn cluster in the S_2 state, which is not consistent with the value of approximately 0.2 ms measured by Lorigan and Britt (1994) at this temperature. More recently, Kodera et al. (1994) have used a pulsed EPR selective hole-burning method and Un et al. (1994) have used 245-GHz EPR line shape analysis to obtain estimates of the distance between $Y_D^{\bullet}$ and the Mn cluster of 28−30 and 25−35 Å, respectively. However, these novel methods have not yet been applied to systems in which the distances and magnetic properties are well-characterized.

There is growing evidence for a structural homology between the PSII reaction center core and the structurally-characterized reaction center from purple bacteria (Michel & Deisenhofer, 1988). For example, Y_D and Y_Z were shown to be symmetrically located in PSII at a distance of 37 Å from the nonheme Fe^{2+} (Kouloughliotis et al., 1995). These results agree well with the predicted C_2 symmetric location of the two tyrosines and their distance from the nonheme Fe^{2+} in computer models of the structure of the D1/D2 complex based on the structure of the bacterial reaction center (Svensson et al., 1990). The distance between Y_D and Y_Z has also been estimated to be about 33 Å from computer models of the structure of the D1/D2 complex (Svensson et al., 1990). However, the Mn cluster is unique to PSII and its location within the PSII complex remains unknown. In a recent spin-echo-detected ENDOR spectroscopic study, a distance of approximately 4.5 Å was estimated between Y_Z and the Mn cluster (Gilchrist et al., 1995). Because of the steep r^{-6} dependence of the dipolar interaction, this short distance estimate is probably skewed toward an edge-to-edge distance; adding the size of the two species would give a center-to-center distance of approximately 5−7 Å. The combined distances of approximately 5−7 Å between Y_Z and the Mn cluster and 33 Å between Y_D and Y_Z lead to the prediction that the distance between Y_D and the Mn cluster is in the range 26−40 Å. The distance of greater than 22 Å between Y_D and the Mn cluster determined through our

measurements, together with the estimate of 4.5 Å for the distance between Y_Z and the Mn cluster (Gilchrist et al., 1995), is consistent with the accumulating experimental evidence [reviewed in Debus (1992) and Rutherford et al. (1992)] for the closer association of the Mn cluster with the D1 rather than the D2 subunit of the PSII reaction center.

We have also used saturation−recovery EPR and progressive microwave-power saturation to study the magnetic properties of the altered S_2-state multiline EPR signal species in NH_3-treated PSII. These experiments showed that the two forms of the S_2-state multiline EPR signal species have very similar magnetic properties. Simulations of the two different multiline EPR signals have been performed in the past and it was proposed that the NH_3-modified signal can be explained by stabilization of a new ground spin state of the Mn cluster (Dismukes et al., 1992; Zheng & Dismukes, 1992). A qualitatively similar conclusion was also reached in the study of Belinskii (1994). This proposal could be reconciled with our findings, if we assume that the rearrangement that produces the new ground spin state also results in an energy of the first excited spin state that remains coincidentally about 30 cm^{-1} above the ground state. On the other hand, based on our results, it is probable that the significantly reduced hyperfine splittings of the NH_3-modified S_2-state multiline EPR signal are not due to a dramatic change of the exchange couplings between the Mn atoms.

REFERENCES

Aasa, R., Andréasson, L.-E., Lagenfelt, G., & Vänngård, T. (1987) *FEBS Lett. 221*, 245−248.

Abragam, A. (1955) *Phys. Rev. 98*, 1729−1735.

Abragam, A. (1961) *The Principles of Nuclear Magnetism*, Clarendon Press, Oxford.

Åhrling, K. A., & Pace, R. J. (1995) *Biophys. J. 68*, 2081−2090.

Astashkin, A. V., Kodera, Y., & Kawamori, A. (1994) *J. Magn. Reson. 105*, 113−119.

Beck, W. F., & Brudvig, G. W. (1986) *Biochemistry 25*, 6479−6486.

Beck, W. F., de Paula, J. C., & Brudvig, G. W. (1985) *Biochemistry 24*, 3035−3043.

Beck, W. F., de Paula, J. C., & Brudvig, G. W. (1986) *J. Am. Chem. Soc. 108*, 4018−4022.

Beck, W. F., Innes, J. B., & Brudvig, G. W. (1990) in *Current Research in Photosynthesis* (Baltscheffsky, M., Ed.) Vol. 1, pp 817−820, Kluwer Academic Publishers, Dordrecht, The Netherlands.

Beck, W. F., Innes, J. B., Lynch, J. B., & Brudvig, G. W. (1991) *J. Magn. Reson. 91*, 12−29.

Beinert, H., & Orme-Johnson, W. H. (1967) in *Magnetic Resonance in Biological Systems* (Ehrenberg, A., Malmström, B. G., and Vänngård, T., Eds.) pp 221−247, Pergamon Press, Oxford.

Belinskii, M. I. (1994) *Chem. Phys. 189*, 451−465.

Bloembergen, N. (1949) *Physica 15*, 386−426.

Bosch, M. K., Evelo, R. G., Styring, S., Rutherford, A. W., & Hoff, A. J. (1991) *FEBS Lett. 292*, 279−283.

Boussac, A., & Rutherford, A. W. (1988) *Biochemistry 27*, 3476−3483.

Boussac, A., & Rutherford, A. W. (1994) *J. Biol. Chem. 269*, 12467−12462.

Boussac, A., Zimmermann, J.-L., & Rutherford, A. W. (1989) *Biochemistry 28*, 8984−8989.

Britt, R. D., Zimmermann, J.-L., Sauer, K., & Klein, M. (1989) *J. Am. Chem. Soc. 111*, 3522−3532.

Britt, R. D., Lorigan, G. A., Sauer, K., Klein, M. P., & Zimmermann, J.-L. (1992) *Biochim. Biophys. Acta 1040*, 95−101.

Castner, T. G., Jr. (1959) *Phys. Rev. 115*, 1506−1515.

Cheniae, G. M., & Martin, I. F. (1970) *Biochim. Biophys. Acta 197*, 219−239.

Debus, R. J. (1992) *Biochim. Biophys. Acta 1102*, 269−352.

de Groot, A., Plijter, J. J., Evelo, R., Babcock, G. T., & Hoff, A. J. (1986) *Biochim. Biophys. Acta 848*, 8−15.

de Paula, J. C., & Brudvig, G. W. (1985) *J. Am. Chem. Soc. 107*, 2643−2648.

de Paula, J. C., Innes, J. B., & Brudvig, G. W. (1985) *Biochemistry 24*, 8114−8120.

de Paula, J. C., Beck, W. F., & Brudvig, G. W. (1986) *J. Am. Chem. Soc. 108*, 4002−4009.

DeRose, V. J., & Hoffman, B. M. (1995) *Methods Enzymol. 246*, 554−589.

Dismukes, G. C., & Siderer, Y. (1981) *Proc. Natl. Acad. Sci. U.S.A. 78*, 274−278.

Dismukes, G. C., Tang, X., Khangulov, S. V., Sivaraja, M., & Pessiki, P. (1992) in *Research in Photosynthesis* (Murata, N., Ed.) pp 257−264, Kluwer Academic Publishers, Dordrecht, The Netherlands.

Evelo, R. G., & Hoff, A. J. (1991) *J. Magn. Reson. 95*, 495−508.

Evelo, R. G., Styring, S., Rutherford, A. W., & Hoff, A. J. (1989) *Biochim. Biophys. Acta 973*, 428−442.

Falkowski, K. M., Scholes, C. P., & Taylor, H. (1986) *J. Magn. Reson. 68*, 453−468.

Galli, C., Atta, M., Andersson, K. K., Gräslund, A., & Brudvig, G. W. (1994) *J. Am. Chem. Soc. 117*, 740−746.

Galli, C., Innes, J. B., Hirsh, D. J., & Brudvig, G. W. (1996) *J. Magn. Reson. B110*, 284−287.

Gilchrist, M. L. J., Ball, J. A., Randall, D. W., & Britt, R. D. (1995) *Proc. Natl. Acad. Sci. U.S.A. 92*, 9545−9549.

Goldberg, D. P., Koulougliotis, D., Brudvig, G. W., & Lippard, S. J. (1995) *J. Am. Chem. Soc. 117*, 3134−3144.

Haddy, A., Aasa, R., & Andréasson, L.-E. (1989) *Biochemistry 28*, 6954−6959.

Haddy, A., Waldo, G. S., Sands, R. H., & Penner-Hahn, J. E. (1994) *Inorg. Chem. 33*, 2677−2682.

Hansson, Ö., & Andréasson, L.-E. (1982) *Biochim. Biophys. Acta 679*, 261−268.

Hansson, Ö., Andréasson, L.-E., & Vänngård, T. (1984) in *Advances in Photosynthesis Research* (Sybesma, C., Ed.) Vol. 1, pp 307−310, Martinus Nijhoff/Dr. W. Junk Publishers, The Hague, The Netherlands.

Hansson, Ö., Aasa, R., & Vänngård, T. (1987) *Biophys. J. 51*, 825−832.

Hirsh, D. J., Beck, W. F., Innes, J. B., & Brudvig, G. W. (1992a) *Biochemistry 31*, 532−541.

Hirsh, D. J., Beck, W. F., Lynch, J. B., Que, L., Jr., & Brudvig, G. W. (1992b) *J. Am. Chem. Soc. 114*, 7475−7481.

Innes, J. B., & Brudvig, G. W. (1989) *Biochemistry 28*, 1116−1125.

Kim, D. H., Britt, R. D., Klein, M. P., & Sauer, K. J. (1990) *J. Am. Chem. Soc. 112*, 9389−9391.

Kim, D. H., Britt, R. D., Klein, M. P., & Sauer, K. (1992) *Biochemistry 31*, 541−547.

Kodera, Y., Takura, K., & Kawamori, A. (1992) *Biochim. Biophys. Acta 1101*, 23−32.

Kodera, Y., Dzuba, S. A., Hara, H., & Kawamori, A. (1994) *Biochim. Biophys. Acta 1186*, 91−99.

Kok, B., Forbush, B., & McGloin, M. (1970) *Photochem. Photobiol. 11*, 457−475.

Koulougliotis, D. (1995) Ph.D. Thesis, Yale University, New Haven, CT.

Koulougliotis, D., Hirsh, D. J., & Brudvig, G. W. (1992) *J. Am. Chem. Soc. 114*, 8322−8323.

Koulougliotis, D., Innes, J. B., & Brudvig, G. W. (1994) *Biochemistry 33*, 11814−11822.

Koulougliotis, D., Tang, X., Diner, B. A., & Brudvig, G. W. (1995) *Biochemistry 34*, 2850−2856.

Lorigan, G. A., & Britt, R. D. (1994) *Biochemistry 33*, 12072−12076.

Michel, H., & Deisenhofer, J. (1988) *Biochemistry 27*, 1−7.

Miller, A.-F., & Brudvig, G. W. (1991) *Biochim. Biophys. Acta 1056*, 1−18.

Murata, N., Miyao, M., Omata, T., Matsunami, H., & Kuwabara, T. (1984) *Biochim. Biophys. Acta. 765*, 363−369.

Nakagawa, K., Candelaria, M. B., Chik, W. W. C., Eaton, S. S., & Eaton, G. R. (1992) *J. Magn. Reson. 98*, 81−91.

Orbach, R. (1961a) *Proc. R. Soc. London, Ser. A 264*, 458−484.

Orbach, R. (1961b) *Proc. R. Soc. London, Ser. A 264*, 485−495.
Pace, R. J., Smith, P., Bramley, R., & Stehlik, D. (1991) *Biochim. Biophys. Acta 1058*, 161−170.
Portis, A. M. (1953) *Phys. Rev. 91*, 1071−1078.
Rakowsky, M. H., More, K. M., Kulikov, A. V., Eaton, G. R., & Eaton, S. S. (1995) *J. Am. Chem. Soc. 117*, 2049−2057.
Rupp, H., Rao, K. K., Hall, D. O., & Cammack, R. (1978) *Biochim. Biophys. Acta 537*, 255−269.
Rutherford, A. W. (1985) *Biochim. Biophys. Acta 807*, 189−201.
Rutherford, A. W., Zimmermann, J.-L., & Boussac, A. (1992) in *The Photosystems: Structure, Function and Molecular Biology* (Barber, J., Ed.) pp 179−229, Elsevier Science Publishers, Amsterdam, The Netherlands.
Styring, S., & Rutherford, A. W. (1987) *Biochemistry 26*, 2401−2405.
Styring, S., & Rutherford, A. W. (1988) *Biochemistry 27*, 4915−4923.
Svensson, B., Vass, I., Cedergren, E., & Styring, S. (1990) *EMBO J. 9*, 2051−2059.
Thompson, L. K., & Brudvig, G. W. (1988) *Biochemistry 27*, 6653−6658.
Un, S., Brunel, L.-C., Brill, T. M., Zimmermann, J.-L., & Rutherford, A. W. (1994) *Proc. Nat. Acad. Sci. U.S.A. 91*, 5262−5256.
Van Vleck, J. H. (1940) *Phys. Rev. 57*, 426−447.
Vermaas, W. J. F., Renger, G., & Dohnt, G. (1984) *Biochim. Biophys. Acta 764*, 194−202.
Yocum, C. F., Yerkes, C. T., Blankenship, R. E., Sharp, R. R., & Babcock, G. T. (1981) *Proc. Nat. Acad. Sci. U.S.A. 78*, 7507−7511.
Zheng, M., & Dismukes, G. C. (1992) in *Research in Photosynthesis* (Murata, N., Ed.) Vol. 2, pp 305−308, Kluwer Academic Publishers, Dordrecht, The Netherlands.
Zimmermann, J.-L., & Rutherford, A. W. (1986) *Biochemistry 25*, 4609−4614.
Zimmermann, J.-L., Boussac, A., & Rutherford, A. W. (1993) *Biochemistry 32*, 4831−4841.

BI970326T